HIGH PERFORMANCE LUMPED COMPONENT WILKINSON POWER COMBINER DISTRIBUTED AMPLIFIER DESIGN

by

PRAGASH SANGARAN

Thesis submitted in fulfillment of the requirement
for the degree of
Master of Science

December 2009

ACKNOWLEDGEMENT

First of all, I would like to thank God, the Almighty, for having made everything possible by giving me strength and courage to complete my research and to produce this dissertation successfully. You have given me the power to believe in my passion and pursue my dreams. I could never have done this without the faith I have in you, the Almighty.

I would like to thank my supervisor Dr. Mohd Fadzil Ain for his support, continuous guidance, meticulous suggestions and astute criticism during the practical phase and for his inexhaustible patience during the correction phase of this dissertation.

I would also like to express my sincere gratitude to all staffs in the school of Electrical & Electronic Engineering of USM Transkrian as well as the Institute of Graduate Studies (IPS) in the USM main campus for their administrative support throughout my Masters programme. My sincere thanks also goes to Motorola for providing education assistance (EA) to support my expenses for semester fees and books.

I would like to thank my mentor Mr. Narendra Kumar for his precious guidance and moral support throughout every stage of the project. He had always played a key role in encouraging me throughout this whole project and keeping me abreast with the scientific developments in the Electrical & Electronic engineering field. Mr. Narendra

Kumar was always there giving helping hands every time I encounter technical issues related to distributed amplifier theory and Advance Design System (ADS).

My sincere thanks to my friend Mr. Lokesh Anand for his guidance and help in submitting technical papers. His help and guidance is essential for my success in submitting papers for conferences.

Thanks to all the people who were involved directly or indirectly in my research and this thesis writing.

To my beloved family; my late father, my mother and brother, I can barely find the words to express all the wisdom, love and support you all have given me. I love you all.

TABLE OF CONTENTS

CHAPTER 3 – PROBLEM STATEMENT AND METHODOLOGY

CHAPTER 4 – DESIGN AND SIMULATION RESULTS

LIST OF TABLES

LIST OF FIGURES

LIST OF ABBREVIATIONS

DA	Distributed Amplifier
VHF	Very High Frequency
UHF	Ultra High Frequency
PAE	Power Added Efficiency
LC	Lumped Component
STAN	Stability Analysis
PCB	Printed Circuit Board
PA	Power Amplifier
RF	Radio Frequency
MOSFET	Metal Oxide Semiconductor Field Effect Transistor
CMOS	Complementary Metal Oxide Semiconductor
NMOS	N Channel Metal Oxide Semiconductor
AC	Alternating Current
DUT	Device Under Test
DAT	Distributive Active Transformer
FET	Field Effect Transistor
DC	Direct Current
BJT	Bipolar Junction Transistor
GaAs	Gallium Arsenide
HBT	Heterojunction Bipolar Transistor
ADS	Advance Design System
ESR	Equivalent Series Resistance

RCL	Resistor Capacitor Inductor
RFIC	Radio Frequency Integrated Circuit
W	width
t	thickness
ε_r	dielectric constant
Wg	Gap Width

LIST OF PUBLICATION

1. Narendra. K, M. F. Ain, L. Anand, P. Sangaran and S. I. Hassan, “High Efficiency applying drain impedance tapering for 600mW pHEMT Distributed Power Amplifier”, *IEEE International Conference on Microwave and Millimeter Wave Technology*, 2008.

REKABENTUK PENGUAT TERAGIH PENGGABUNG KUASA WILKINSON KOMPONEN TERGUMPAL BERPRESTASI TINGGI

ABSTRAK

Perkembangan penguat kuasa jalur lebar adalah penting untuk teknologi radio pada masa depan. Penguat kuasa jalur lebar konvensional mempunyai produk gandaan-lebar jalur lebar yang terbatas berdasarkan transistor yang digunakan. Penguat teragih mampu menangani masalah ini melalui gabungan kuasa output daripada pelbagai transistor. Walau bagaimanapun, penguat kuasa jalur lebar konvensional juga mempunyai jalur lebar yang terbatas. Tambahan peranti yang melebihi jumlah optimum akan meningkatkan get dan mengecilkan 'drain line', dan seterusnya akan mengurangkan prestasi kuasa. Di samping itu, penguat teragih konvensional juga memaparkan kuasa dan kecekapan yang rendah disebabkan gelombang berbalik daripada 'drain line'. Dalam projek ini, penggabung dan pelerai kuasa komponen tergumpal Wilkinson digunakan pada input dan output setiap penguat teragih untuk meningkatkan jalur lebar, kecekapan dan kuasa output daripada penguat teragih. Penguat teragih penggabung kuasa komponen tergumpal Wilkinson dan penguat kuasa jalur lebar konvensional direka bentuk. Prestasi penguat teragih penggabung kuasa komponen tergumpal Wilkinson dan penguat kuasa jalur lebar konvensional dibandingkan dengan mengunakan bilangan peranti yang sama, susun atur dan bekalan arus terus. Prestasi hasil ukuran peguat kuasa ini mempunyai jalur lebar dari 100 MHz sehingga 610 MHz dan dari 100 MHz sehingga 520 MHz dengan masing-masing kuasa output 26.25 dBm sehingga 29.56 dBm and 24.11 dBm sehingga 28.51 dBm. "Power

added efficiency” (PAE) bagi penguat teragih penggabung kuasa komponen tergumpal Wilkinson ialah daripada 26.2 % sehingga 36 % manakala PAE bagi penguat kuasa jalur lebar konvensional ialah daripada 20.5 % sehingga 26.5 %. Penguat ini difabrikasikan pada papan tercetak litar berketebalan 14 mil dengan pemalar dielektrik 4.5. Hasil ukuran daripada fabrikasi dibandingkan dengan keputusan simulasi dan didapati hampir dengan keputusan simulasi.

.

HIGH PERFORMANCE LUMPED COMPONENT WILKINSON POWER COMBINER DISTRIBUTED AMPLIFIER

ABSTRACT

The development of broadband power amplifier is critical for future radio technology. Conventional broadband power amplifier has gain-bandwidth product limitation based on transistor used. Distributed amplifier (DA) overcomes this limitation by combining output power from several transistors in additive fashion. However, conventional distributed amplifier has limitation in bandwidth as well. Adding devices beyond optimum number will increase gate and drain line attenuation and will degrade the power performance. Moreover, conventional distributed amplifier also exhibits low power and efficiency due to the drain line reverse wave. In this project, lumped component Wilkinson power combiner and splitter is used at the input and output of the distributed amplifier respectively to increase the bandwidth, efficiency and output power of a distributed amplifier. A lumped component Wilkinson combiner distributed amplifier and a conventional distributed amplifier have been designed. The measured performance of this novel lumped component Wilkinson combiner distributed amplifier had been compared with the conventional distributed amplifier using the same number of devices, layout and dc supply. These amplifiers have frequency range from 100 MHz up to 610 MHz and from 100 MHz to 520 MHz with output power of 26.25 dBm to 29.56 dBm and 24.11 dBm to 28.51 dBm respectively. PAE of LC Wilkinson combiner DA is varies from 26.2 % to 36 % whereas PAE of conventional DA is varies from 20.5 % to 26.5 %. The amplifier had been fabricated on a 14-mil thick printed circuit board

(PCB) with a dielectric constant of 4.5. Measured results of the fabricated board have been found to be comparable to simulation results.

CHAPTER 1
INTRODUCTION

1.1 Background

Current practice is to design single band two-way radios such as VHF (very high frequency) and UHF (ultra high frequency). However future technology is driving towards broadband two-way radio which gives freedom to select the operating frequency band. This will also enable user to communicate with wide range of people. For an example, in the US, the Virginia state police and Georgia state police use different radio frequencies which are 136 MHz (VHF) and 406 MHz (UHF) respectively. So, these two departments can't communicate with each other. In order to communicate, Virginia state police needs to use UHF radio or Georgia state police needs to use VHF radio. Broadband radios are able to offer effective solution for this problem.

The rapid development of broadband systems has created an increasing demand for use of wideband amplifiers. No other amplifier currently can beat the wide band characteristic of the DA. Wide bandwidth, moderate gain and small delay of DAs make them an attractive choice for such applications. However, there are tradeoffs for these advantages. DA is suffering from low efficiency and low output power.

The major challenge is to design high power, high gain, high PAE and broadband DA. Only few works have demonstrated high efficiency with DA topology while preserving reasonable gain. By tapering impedance at drain transmission line and

selecting the device for correct load impedance, dramatic improvement in PAE (almost twice higher then previously reported) can be achieved (Zhao et al., 2002 and 2003). A novel tapered drain line DA had been realized which improve the PAE by 11% to 24% across the 4.5 GHz and also exhibits significant improvement in output power (Shastry et al., 2006).

Few publications have been published based on a technique to merge power combiner and DA in order to improve the large and small signal performance. Eric S. Shapiro has published novel power combiner traveling wave power amplifier design method to improve efficiency by reducing backward wave propagation at the drain transmission line (Shapiro et al., 1998). S. D'Agostino and C. Paoloni have published few publications by employing Wilkinson combiner or splitter (D'Agostino et al., 1995), lange couplers (D'Agostino et al., 1994) and interdigital combiner or splitter (D'Agostino et al., 1995) at the output and input of the DA. The interdigital combiner or splitter was found able to improve the small signal and power performance of the DA is improved as compared to the conventional structure. In (D'Agostino et al., 1994), remarkable improvements in the output power, PAE, and small-signal gain are demonstrated by comparison with the conventional DA topology. From (D'Agostino et al., 1995), small signal gain and power performance has been increased.

Microstrip Wilkinson power combiner and splitter design has been converted to lumped component Wilkinson power combiner and splitter by referring to work by Fernando Noriega (2002).

1.2 Objectives

The objectives of this thesis are listed below:

- To demonstrate detail design methodology of conventional distributed power amplifier (conventional DA).
- To demonstrate a lumped component Wilkinson power combiner DA (LC Wilkinson power combiner DA) design technique by employing lumped component Wilkinson power combiner and splitter at the output and input of the conventional DA respectively.
- Stability analysis of novel DA using STAN (pole-zero identification technique).
- PCB board fabrication and measurement of these two types of power amplifier using same device (Mitsubishi RF MOSFET, RD01MUS1), same bias voltage and same layout (for DA part) to compare their performance in terms of bandwidth and efficiency.

1.3 Thesis Outline

In Chapter 2, literature review is presented. It contains previous related research done by other researchers. Research on conventional DA, power combining techniques, LC Wilkinson combiner DA, and large signal stability analysis has been reviewed.

Chapter 3 discusses briefly the design methodology of conventional DA and LC Wilkinson combiner DA. Measurement setup of PAE, gain and output power also discussed in this Chapter.

Chapter 4 explains design steps of conventional DA and LC Wilkinson combiner DA in detail. Simulation results are also given in this Chapter.

Chapter 5 contains layout guidelines and consideration which has been followed in the design to obtain measured results from fabricated board which is close to simulated results.

Chapter 6 exhibits measurement results of large signal parameters for LC Wilkinson combiner DA and conventional DA and correlation analysis with simulation.

Chapter 7 consists of conclusion and future work.

CHAPTER 2
LITERATURE REVIEW

2.1 Introduction

Power amplifiers (PA) are the heart of the transmitter system. PA is responsible to amplify a signal to the desired power level to be delivered to the load. PA must deliver enough power so that the signal, after path loss, can still be detected by the receiver system.

There are many types of amplifier available. However, only wideband amplifier is of interest for broadband application. The most popular and widely used broadband power amplifier in either discrete or monolithic technologies is the DA.

2.2 Distributed Amplification

The concept of traveling wave or distributed amplification has been around for over half century. The term "DA" originated in a paper by Ginzton in 1948 (Ginzton et al., 1948) However, the underlying concepts can be traced back to a patent by Percival in 1937 (Percival et al., 1937).

DAs employ a topology in which the gain stages are connected such that their capacitances are separated, yet the output currents still combine in an additive fashion. Series-inductive elements are used to separate capacitances at the input and output of adjacent gain stages. The resulting topology, given by the interlaying series inductors and shunt capacitances, forms what is essentially a lumped components artificial

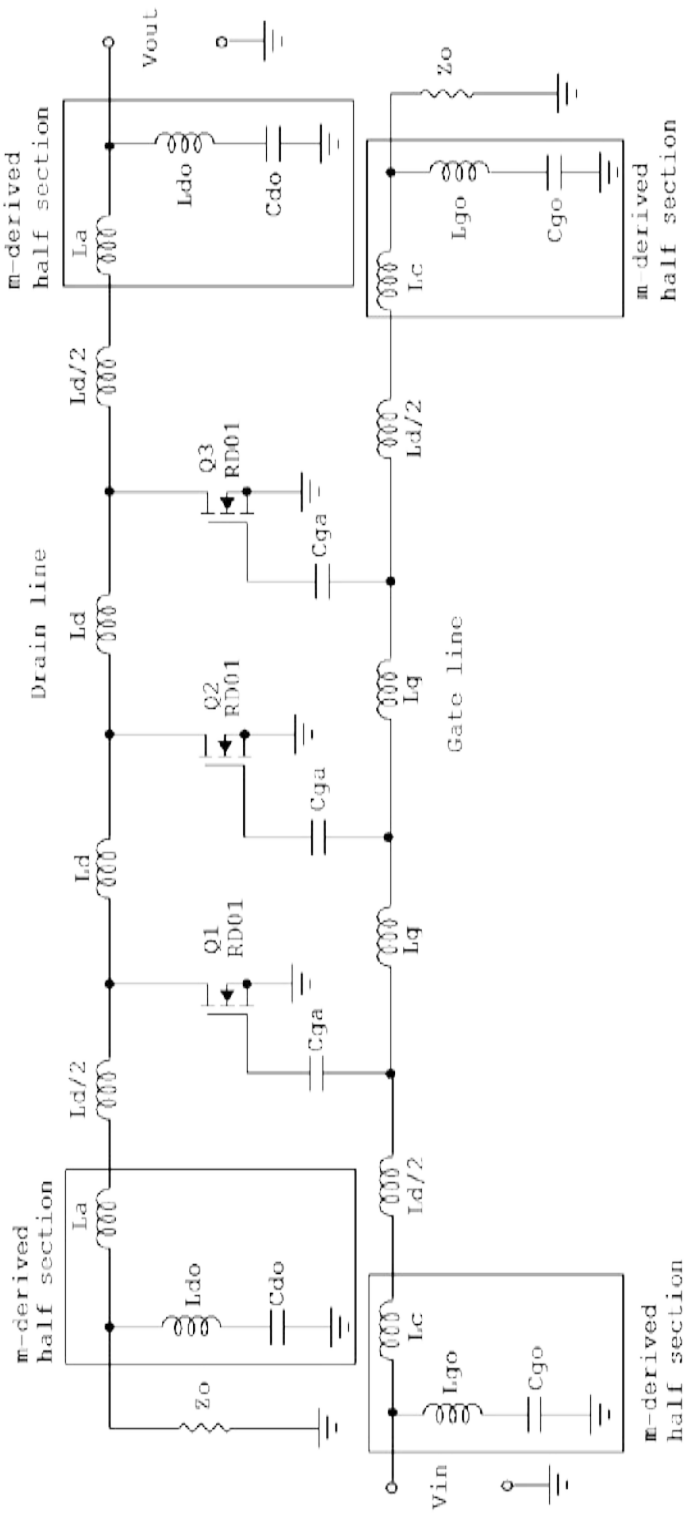

Figure 2.1: Conventional LDMOS (RD01MUS1) 3-stage DA topology.

transmission line as shown in Figure 2.1. The additive nature of the gain dictates a

relatively low gain. However, the distributed nature of the capacitance allows the amplifier to achieve very wide bandwidths.

2.2.1 Theoretical Analysis

2.2.1.1 Introduction

Analysis of DAs is facilitated by the assumption of lossless transmission networks which are realized from ladder networks based on constant k low pass filters, and unilateral active devices.

The DA concept has been successfully applied to monolithic GaAs MESFET amplifiers at microwave frequencies in the 80's for larger gain-bandwidth products. Ayasli have published design method of traveling wave amplifier based on an approach that approximates gate and drain lines as continuous structures (Ayasli et al., 1982). Similarly, Beyer developed a closed form expression for the gain that depends on the circuit's propagation constants and the gate circuit cut-off frequency (Beyer et al., 1984). Niclas has also developed a method based on the use of the admittance matrix employing the Y parameters of the transistor model in an amplifier with either artificial or real transmission lines (Niclas et al., 1983). This method allows the use of much more sophisticated model for the transistor developed from its measured S parameters. McKay proposed also a formulation based on a normalized transmission using matrix formulation (McKay et al., 1986). This technique yields insight into amplifier operation because it displays the traveling-wave nature of a DA.

2.2.1.2 Concept of Distributed Amplification

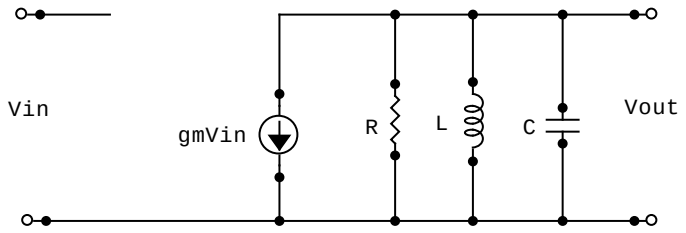

Figure 2.2: A simple band pass amplifier (Wong., 1993).

Gain and bandwidth of an amplifier cannot be simultaneously increased beyond a certain limit (Wong., 1993). Figure 2.2 shows a simple band pass amplifier consisting of an active device and a resonant coupling circuit.

The voltage transfer function of this amplifier can be written as (Wong., 1993):

$$A_v(\omega) = \frac{-g_m R}{1 + jQ\left(\frac{\omega}{\omega_0} - \frac{\omega_0}{\omega}\right)} \tag{2.1}$$

g_m is device transconductance, R, L and C are resistor, inductor and capacitor of the low pass filter, respectively. ω_0 is the low pass filter cut-off frequency, ω is th operating frequency and Q is the quality factor. $\omega_0 = 1/(LC)^{1/2}$ and $Q = \omega_0 RC$. The maximum gain occurs at mid band and has a magnitude of $g_m R$. The bandwidth, B is $\omega_0/(2\pi Q)$. Hence, the gain-bandwidth product of the amplifier, $A_{v0}B$, is given as (Wong., 1993):

$$A_{v0}B = \frac{g_m}{2\pi C} \tag{2.2}$$

in Hz.

This limitation may never be surpassed by an optimization of external circuit elements. Any increase in gain will be offset by a reduction of the same amount in the bandwidth (Wong., 1993).

Obviously this gain-bandwidth limitation cannot be overcome by connecting devices in parallel because both the transcoductance and the capacitance will be multiplied by the same amount so that their ratio remains the same.

Considering a network theorem first proposed by Bode in 1945, an upper limit to the gain-bandwidth product could be found. The theorem states that given an impedance function Z(ω) and defining a + jb = log Z, where a and b are functions of ω, then (Wong., 1993):

$$\int_0^1 \frac{a(\omega)}{\sqrt{1-\omega^2/\omega_c^2}}\, d\left(\frac{\omega}{\omega_c}\right) \le \frac{\pi}{2}\log\left(\frac{2}{\omega_c C}\right) \tag{2.3}$$

with the equality sign holding when (Wong., 1993):

$$Z = \left[\frac{1}{2} \left(\sqrt{\omega_c^2 - \omega^2} + j\omega \right) C \right]^{-1} \tag{2.4}$$

where C is(Wong., 1993):

$$C = \lim_{\omega \to \infty} \frac{1}{j\omega Z} \tag{2.5}$$

and implies that the impedance Z becomes capacitive in the high-frequency limit, where capacitance is denoted by C.

Now, considering an active device with an output termination of Z(ω), which accounts for the intrinsic shunting elements inherent to the output characteristics of the active device, stray capacitance, and other additional passive circuit elements introduced to form the coupling circuit, the voltage gain related to a on a logarithmic scale is (Wong., 1993):

$$\log|A_v| = \log g_m + \log|Z| = \log g_m + a \tag{2.6}$$

where g_m is the transcondutance of the device.

Since the weighted sum on the left-hand side of Equation 2.3 is maximum when Z is given by Equation 2.4, for which a=log(2/Cw$_c$), it follows that the maximum uniform gain in logarithm is given as (Wong., 1993):

$$Gain = \log g_m + \log \frac{2}{C\omega_c} \tag{2.7}$$

over the frequency range from 0 to ω_c. On linear scale, the maximum uniform gain becomes $2g_m/C\omega_c$.

For a given C, gain can be increased by choosing a small ω_c, however, the product of |Z(0)| and ω_c remains the same with a value of 2/C, hence the maximum gain-bandwidth product obtainable from this amplifier can be obtained as $(2g_m/C\omega_c)(\omega_c/2\pi)=g_m/\pi C$ in hertz.

This important result was first arrived at by Wheeler (1939) and mathematically shown by Bode (1945) and Hansen (1945) by means of analytic function theory and potential analogy.

The required Z(ω) that maximizes gain-bandwidth product of the device is given in the above discussion in Equation 2.4. This impedance can be realized by a low pass constant k-filter terminated with a full-shunt at the diving point, as shown in Figure 2.3.

The impedance Z(ω) has a constant magnitude from zero frequency to ω_c. Since this network is infinite, truncating this network and terminating by an m-derived half section followed by a resistor could approximate this infinite network.

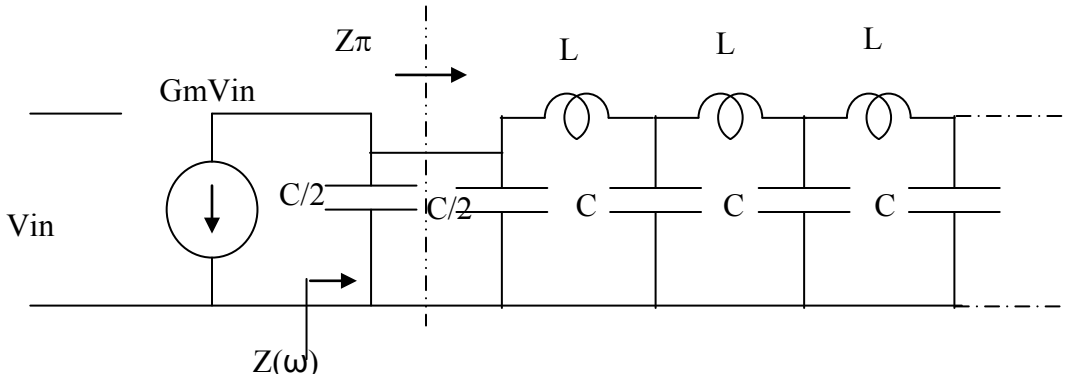

Figure 2.3: Realization of Z(ω) for maximum uniform gain (Wong., 1993).

2.2.2 Image Parameter Method

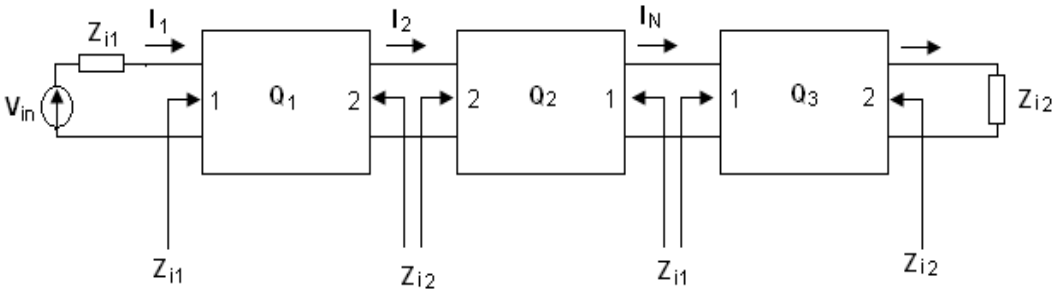

Figure 2.4: Artificial transmission line (Wong., 1993).

The image parameter method applied to the DA since it consists of a cascade of identical two-port networks forming an artificial transmission line. The cascaded two port network is shown in Figure 2.4.

When considering signal transmission and impedance matching in cascaded two-ports, each two-port should operate with the appropriate impedance terminations so that the maximum power transfer takes place over the prescribed bandwidth. Such condition can be met by terminating the two-port with a pair of impedances known as image impedance so that the impedance appears the same when one looks into either direction of each port as shown in Figure 2.5. Those impedances can be expressed as Z_{i1} and Z_{i2}.

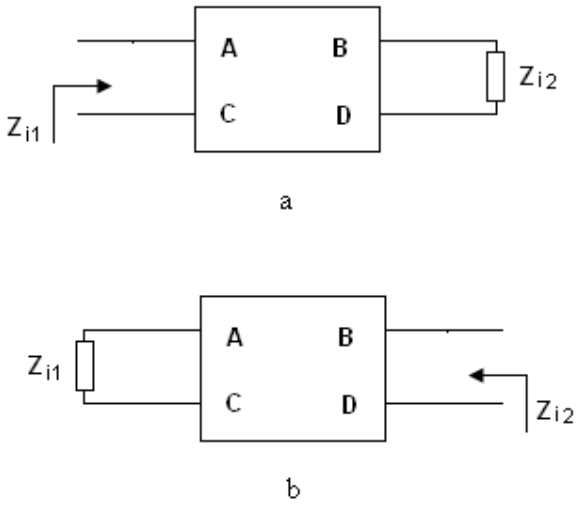

Figure 2.5: A two-port network terminated by its image impedance. (a) Image impedance at port 1 (b) image impedance at port 2 (Wong., 1993).

The image impedance may also be expressed as (Wong., 1993):

$$Z_{i1} = \sqrt{Z_{sc1} Z_{oc1}} = \sqrt{\frac{B}{D}} \sqrt{\frac{A}{C}} \tag{2.8}$$

$$Z_{i2} = \sqrt{Z_{sc2} Z_{oc2}} = \sqrt{\frac{B}{C}} \sqrt{\frac{D}{A}} \tag{2.9}$$

where Z_{sc1} and Z_{oc1} are the impedances appearing at port 1, with port 2 short circuited and open circuited, respectively, and likewise for Z_{i2}. If the network is symmetrical, Z_{i1} and Z_{i2} become identical, known as characteristic impedance and is denoted Z_0.

Figure 2.4 shows the case of an infinite number of identical networks connected so that at each junction either "end 1s" are connected together or "end 2s" are connected together. Because the way the infinite chain of networks in Figure 2.4 is connected, the impedance seen looking left and right at each junction are always equal, hence there is never any reflection of a wave passing through a junction. Thus, from the wave point of view, the networks of the Figure 2.4 are perfectly matched. The image impedance Z_i for a reciprocal symmetric two-port is defined as the impedance looking into port 1 and 2 of the two-port when the other terminal is also terminated in Z_i (Matthaei et al., 1964).

To achieve an impedance match over a broad range, the load and source impedance must be transformed into the image impedance. Otherwise, the gain response will not flat as function of frequency. The low pass m-derived half section shown in Figure 2.6, serves this purpose well (Beyer et al., 1984). The impedance looking into the gate and drain line when transformed by the m-derived section is approximately constant over a broad range of frequencies. The m-derived impedance matching network provides a big improvement of the variations over the broadband frequency. It can also be used to match directly to $Z_o = 50\Omega$. Constant-k and m-derived filters are classic examples of filters designed from the image point of view (Wong., 1993).

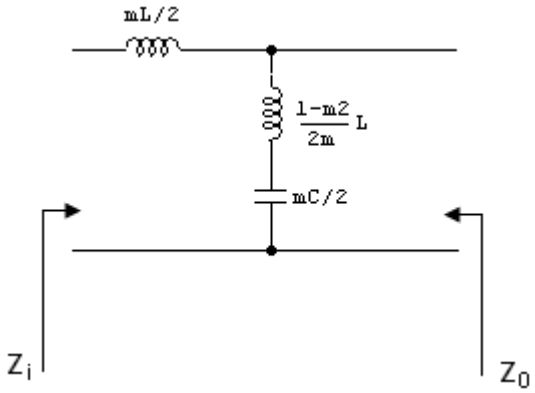

Figure 2.6: Low pass m-derived half section (Wong., 1993).

2.2.3 Two-Port Theory

Large signal model of Silicon RF Power MOSFET as showed in Figure 2.7 published by Paolo Fioravanti et al., is used to model RD01MUS1 (Fioravanti et al., 2007). C_{gd} is gate to drain capacitance, C_{gs} is gate to source capacitance, C_{ds} is drain to

source capacitance and g_m is device transconductance. The device is assumed to be unilateral so C_{gd} is neglected.

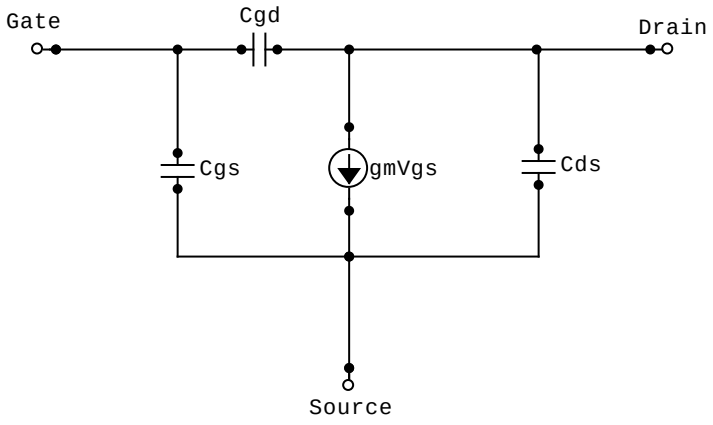

Figure 2.7: Silicon RF power MOSFET bilateral large signal model (Fioravanti et al., 2007).

The DA could be broken down into two main lines: the drain line and the gate line as shown in Figure 2.8. The lines are assumed to be terminated by their image impedances at both ends.

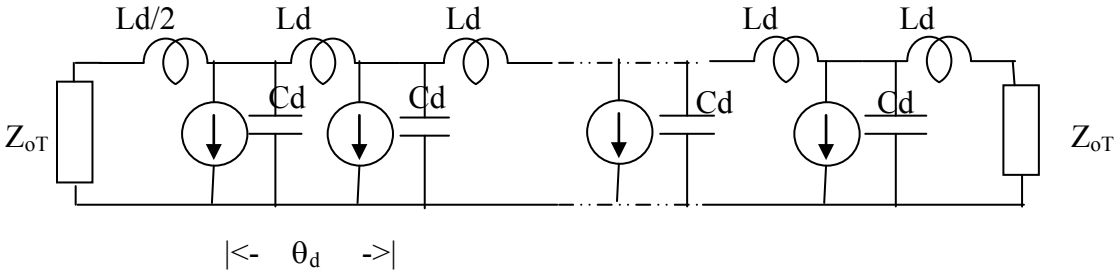

(a)

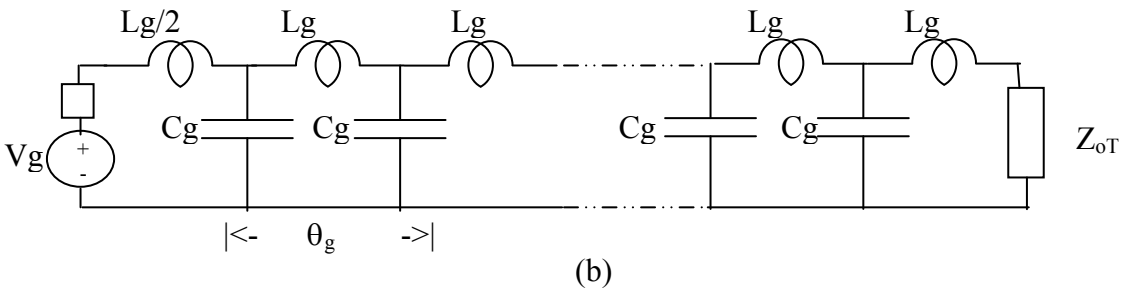

(b)

Figure: 2.8: An ideal DA (a) Drain line (b) Gate line (Wong., 1993).

The two lines are coupled through the action of the transconductance. Signals in the drain line are induced by the signals in the gate line (Beyer et al., 1984). The voltage at a node k of the gate line can be written as (Beyer et al., 1984):

$$V_{gk} = V_{in}\sqrt{\frac{Z_{o\pi}^{g}}{Z_{oT}^{g}}}e^{-(k-1/2)\theta_g} \tag{2.10}$$

At the corresponding location on the drain line, a current I_k will be induced with a value of (Beyer et al., 1984):

$$I_k = -g_m V_{gk} \tag{2.11}$$

By superposition, the voltage developed across Z_{oT} on the drain line can be written as (Beyer et al., 1984):

$$V_{out} = \frac{1}{2}\sqrt{\frac{L}{C}e^{-\theta/2}}\sum_{k=1}^{N} I_k e^{-\theta(N-k)} \tag{2.12}$$

Substituting for the value of I_k from Equation 2.11 in Equation 2.12 yields (Beyer et al., 1984):

$$V_{out} = -\frac{V_{in} g_m}{2} \sqrt{\frac{Z^g_{o\pi}}{Z^g_{oT}}} \sqrt{Z^d_{o\pi} Z^d_{oT}} e^{(\theta_g - \theta_d)/2} e^{-N\theta_d} \sum e^{k(\theta_d - \theta_g)} \qquad (2.13)$$

Assuming that phase synchronization is applied by adding a parallel capacitance to the devices at the drain line, then $\theta_d = \theta_g$, and the voltage gain could be written as (Beyer et al., 1984):

$$A_v = -\frac{N g_m}{2\sqrt{1 - w^2 / w_c^2}} \sqrt{\frac{L_d}{C_d}} e^{-N\theta} \qquad (2.14)$$

Under matched conditions, the signal in the gate line propagates only in one direction. However, waves do propagate in both directions in the drain line. The voltage at the load on the left is a superposition of backward traveling waves which give rise to a highly frequency dependent signal given by (Beyer et al., 1984):

$$V^L_{out} = -\frac{V_{in} g_m}{2\sqrt{1 - w^2 / w_c^2}} \sqrt{\frac{L_d}{C_d}} e^{-N\theta} \frac{\sinh(N\theta)}{\sinh(\theta)} \qquad (2.15)$$

Power gain of a DA could be expressed as (Beyer et al., 1984):

$$G = \frac{P_{out}}{P_{in}} = \frac{N^2 g_m^2}{4(1 - w^2 / w_c^2)} \sqrt{\frac{L_g L_d}{C_g C_d}} e^{-2N\theta} \tag{2.16}$$

2.2.4 Admittance Matrix

The basic circuit of a DA can be represented by four-port as shown in Figure 2.9 (Niclas et al., 1983). Equivalent circuit in the Figure 2.9 can be constructed by replacing the transistor by its two port representation with the current source i_k.

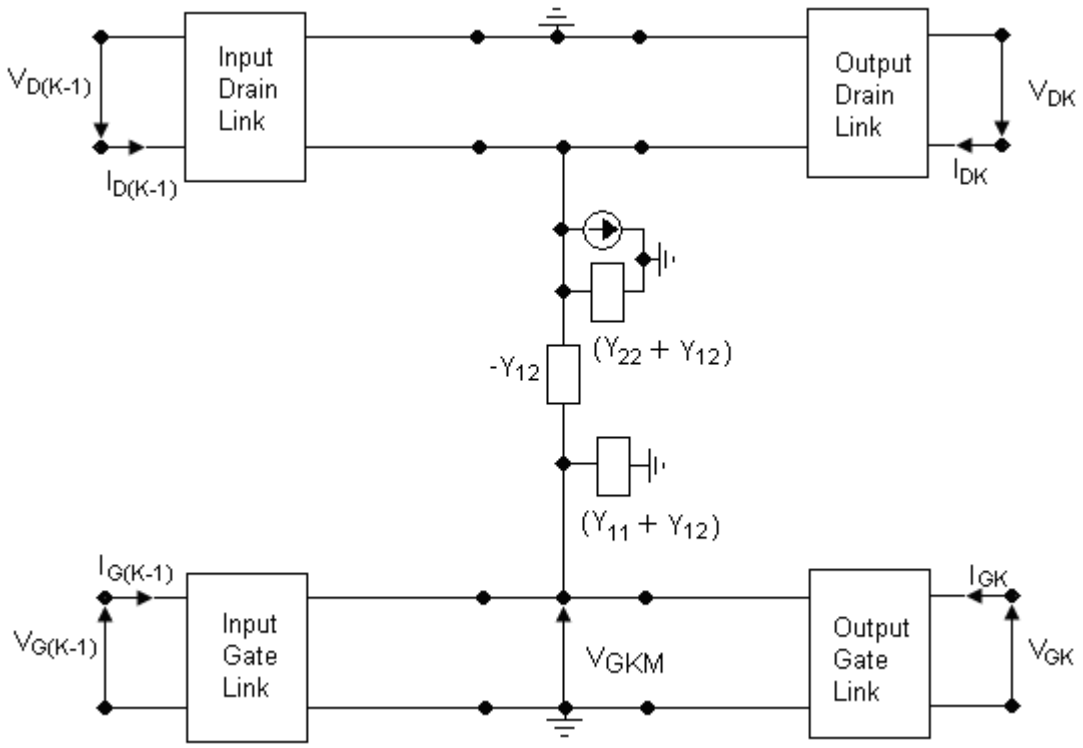

Figure 2.9: Four-port representation of the elementary DA circuit (Niclas et al., 1983).

From Figure 2.9, matrix Equation which relates to the voltage and current can be derived as (Niclas et al., 1983):

$$\begin{bmatrix} V_{Dk-1} \\ I_{Dk-1} \\ V_{Gk-1} \\ I_{Gk-1} \end{bmatrix} = A_k \begin{bmatrix} V_{Dk} \\ -I_{Dk} \\ V_{Gk} \\ -I_{Gk} \end{bmatrix} \tag{2.17}$$

where (Niclas et al., 1983):

$$A_k = A_{1k} A_{Fk} A_{2k} \tag{2.18}$$

$[A_{1k}]$ and $[A_{2k}]$ represent matrix of input and output links respectively (refer to Figure 2.9). $[A_{fk}]$ is represents the MOSFET admittance matrix. Matrix equation as below can be constructed by cascading n elementary circuits and terminating the idle ports with R_G and R_D (the gate and drain loads respectively) (Niclas et al., 1983):

$$\begin{bmatrix} V_{D0} \\ -R_D^{-1} V_{D0} \\ V_{G0} \\ I_{G0} \end{bmatrix} = D \begin{bmatrix} V_{Dn} \\ -I_{Dn} \\ V_{Gn} \\ -R_G^{-1} V_{Gn} \end{bmatrix} \tag{2.19}$$

where (Niclas et al., 1983):

$$D = \prod_{n}^{k=0} A_k \tag{2.20}$$

The insertion gain is the ratio of signal power delivered to the load by the circuit to the signal power delivered directly to that load. The insertion gain can be expressed as (Niclas et al., 1983):

$$Gain = \left| 2Y_0 \frac{C_2}{C} \right| \tag{2.21}$$

with (Niclas et al., 1983):

$$Y_0 = 1/Z_0 \tag{2.22}$$

$$C_1 = D(4,3) + R_G^{-1} D(4,4) + Y_0 (D(3,3) + R_D^{-1} D(3,4)) \tag{2.23}$$

$$C_2 = D(2,3) + R_G^{-1} D(2,4) + Y_0 (D(1,3) + R_D^{-1} D(1,4)) \tag{2.24}$$

$$\begin{aligned} C = {} & C_1 [D(2,1) + Y_0^{-1} D(2,2) + Y_0 (D(1,1) + R_D^{-1} D(1,2))] \\ & - C_2 [D(4,1) + Y_0^{-1} D(4,2) + Y_0 (D(3,1) + R_D^{-1} D(3,2))] \end{aligned} \tag{2.25}$$

The above mentioned solution expresses the gain of the DA in general form. Since for DA, the load and input impedance are the same (50 Ω), insertion gain and transducer gain also will be the same.

2.2.5 Coupled-Wave Analyses

Analysis in section 2.2.3 by James B. Beyer is based on unilateral device models. However, certain aspects of the amplifier and its characteristics cannot be adequately explained by the unilateral active device model such as input-output isolation. A more completed model required to explain these characteristics. This lead to bilateral coupling between input (gate) and output (drain). This can be called as gate drain capacitance (C_{gd}). The equivalent circuit model must be accurate over the frequency band of interest in order to obtain accurate description of DA characteristics.

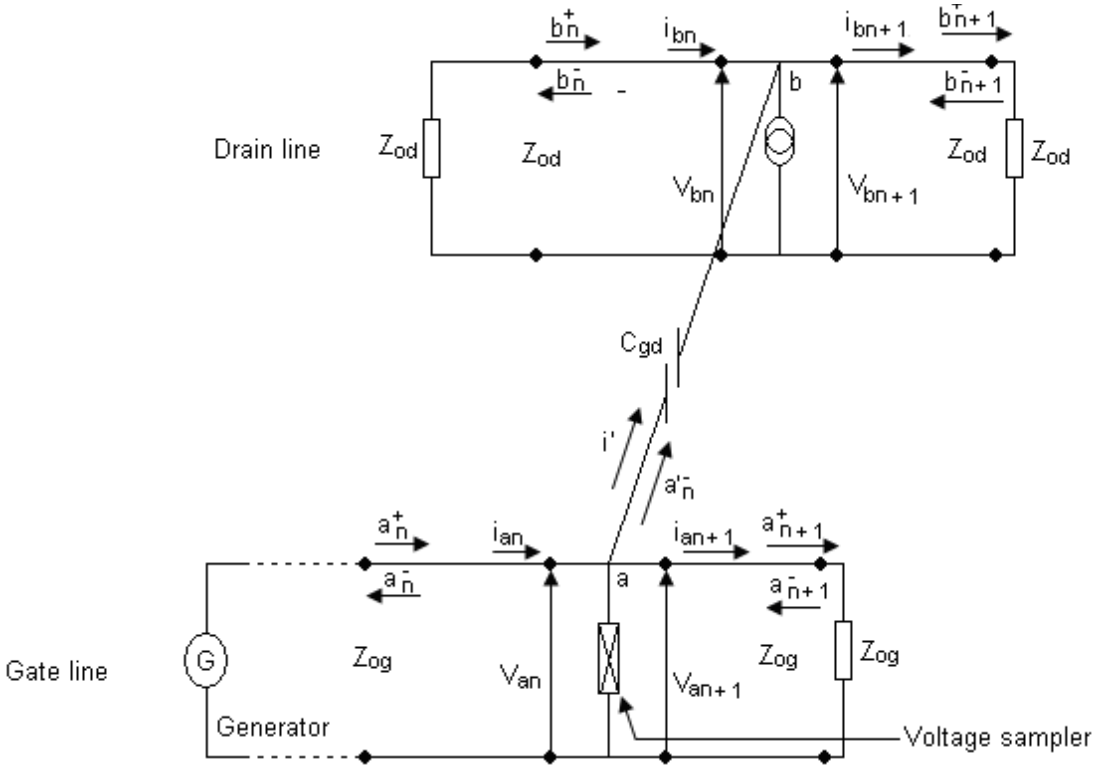

Figure 2.10: Elementary section of a bilateral DA. The variables b_n and a_n represent the scattering waves (Moussa et al., 2003).

The normalized transmission matrix approach was invented by McKay (Mckay et al., 1986). This theory applies to general class of DA with discrete sampling points on the gate line which couple to discrete excitation points on the drain line. Si Moussa (2003) extends this concept by considering the bilateral case obtained by including the C_{gd} of the device.

Using the scattering formalism, the wave quantities as shown in Figure 2.10 are given by (Moussa et al., 2003):

$$b^{\pm}{}_n = \frac{V_{bn}}{\sqrt{Z_{0_d}}} \pm i_{bn}\sqrt{Z_{0_d}} \tag{2.26}$$

$$a^{\pm}{}_n = \frac{V_{a_n}}{\sqrt{Z_{0_g}}} \pm i_{a_n}\sqrt{Z_{0_g}} \tag{2.27}$$

$$a_n^{'-} = (a_n^- + a_{n+1}^+) - \frac{a_n^+ + a_n^-}{2} \tag{2.28}$$

where V_{a_n}, i_{a_n}, V_{b_n} and i_{b_n} are the voltages and currents at section n. The 'a' and 'b' are portrayed the waves on the gate and drain line, respectively. Characteristic impedance of the gate line and drain line is given by Z_{0_g} and Z_{0_d}.

Since (Moussa et al., 2003) $V_{a_{n+1}} = V_{a_n}$,

$$a_n^{'-} = \frac{V_{a_n}}{\sqrt{Z_{0_g}}} - \sqrt{Z_{0_g}}(i_{a_{n+1}} - i_{a_n}) \tag{2.29}$$

The transfer matrix [M] defined as [M] = [G-1/2][T^N][$G_{1/2}$] is given by (M. Si Moussa et al., 2003):

$$W_{out} = [G_{-1/2}][T^N][G_{1/2}]W_{in} \tag{2.30}$$

where (Moussa et al., 2003):

$$W_i = [a_i^+ b_i^+ a_i^- b_i^-]^T \tag{2.31}$$

Where ^{T} denotes the operator transpose, W_{in} and W_{out} are the input and the output vector, respectively (Moussa et al., 2003):

$$[G_{1/2}] = diag\{\exp(-\theta_g), \exp(-\theta_d), \exp(\theta_g), \exp(\theta_d)\} \tag{2.32}$$

$$[H] = \begin{bmatrix} 1 + jZ_{0_g}C_{gd}\omega & -\frac{1}{2}jC_{gd}\omega\sqrt{Z_{0_g}Z_{0_d}} & \frac{1}{2}jZ_{0_g}C_{gd}\omega & -\frac{1}{2}jC_{gd}\omega\sqrt{Z_{0_g}Z_{0_d}} \\ H + \frac{1}{2}jC_{gd}\omega\sqrt{Z_{0_g}Z_{0_d}} & 1 - \frac{1}{2}jZ_{0_d}ZC_{gd}\omega & -H - \frac{1}{2}jC_{gd}\omega\sqrt{Z_{0_g}Z_{0_d}} & -\frac{1}{2}jZ_{0_d}C_{gd}\omega \\ -\frac{1}{2}jZ_{0_g}C_{gd}\omega & \frac{1}{2}jC_{gd}\omega\sqrt{Z_{0_g}Z_{0_d}} & 1 - jZ_{0_g}C_{gd}\omega & \frac{1}{2}jC_{gd}\omega\sqrt{Z_{0_g}Z_{0_d}} \\ -H - \frac{1}{2}jC_{gd}\omega\sqrt{Z_{0_g}Z_{0_d}} & \frac{1}{2}jZ_{0_d}C_{gd}\omega & -H - \frac{1}{2}jC_{gd}\omega\sqrt{Z_{0_g}Z_{0_d}} & 1 + \frac{1}{2}jZ_{0_d}C_{gd}\omega \end{bmatrix} \tag{2.33}$$